Title

Insights from the numerical analysis of axially loaded piles in liquefiable soils

Authors

Sinha, Sumeet K
Ziotopoulou, Katerina
Kutter, Bruce L

Publication Date

2025

DOI

10.1016/j.soildyn.2024.109020

Peer reviewed

Soil Dynamics and Earthquake Engineering 188 (2025) 109020

Contents lists available at ScienceDirect

Soil Dynamics and Earthquake Engineering

journal homepage: www.elsevier.com/locate/soildyn

Insights from the numerical analysis of axially loaded piles in liquefiable soils

Sumeet K. Sinha [a,*], Katerina Ziotopoulou [b], Bruce L. Kutter [b]

[a] Dept. of Civil Engineering, Indian Institute of Technology Delhi, Hauz Khas, New Delhi 110016, India
[b] Dept. of Civil and Environmental Engineering, University of California Davis, One Shields Ave., Davis, CA 95616, USA

ARTICLE INFO

Keywords:
Pile design
Liquefaction
Downdrag
Drag load
Neutral plane
TzQzLiq analysis

ABSTRACT

Axially loaded piles in liquefiable soils can undergo severe settlement due to an earthquake event. During shaking, the settlement is caused by the decreased shaft and tip capacity from excess pore pressures (u_e) generated around the pile. Post shaking, soil settlement from the reconsolidation of liquefied soil surrounding the pile results in the development of additional load (known as drag load), causing downdrag settlement of the pile. Estimating the axial load distribution and pile settlement is essential for designing and evaluating the performance of axially loaded piles in liquefiable soils. In practice, a simplified neutral plane solution method is used, where the liquefied soils are modeled as a consolidating layer without considering the effect of u_e generation/dissipation. A TzQzLiq analysis models the load and settlement response of axially loaded piles in liquefiable soils by accounting for the effect of excess pore pressure (u_e) generation/dissipation on the shaft and tip capacity. This paper presents the deficiencies of the simplified neutral plane method in predicting the drag load as well as the downdrag settlement by comparing it with the TzQzLiq analysis validated with hypergravity model tests. The results show that the drag load and the downdrag settlement predicted by the neutral plane method might be over- or under-estimated depending on the pile load, the rate of u_e dissipation, and the soil settlement. For the cases studied, it was found that most of the pile settlement occurs during shaking due to the decrease in the pile's tip resistance from the development of u_e in the soil surrounding it. While large drag loads develop during reconsolidation, the resulting downdrag settlement is small. While the neutral plane method generally predicted a downdrag settlement comparable to that of the TzQzLiq analysis, it overpredicted drag load and could not predict co-seismic settlement. Finally, the study advocates for the development and use of a displacement-based procedure (accounting for all the mechanisms occurring during and after an earthquake event) such as based on TzQzLiq analysis in accurately evaluating the performance of the pile (i.e., the pile settlement and the maximum load), thus providing an overall safe, efficient, and optimized design.

1. Introduction

Axially loaded piles in liquefiable soils can undergo severe settlement due to an earthquake-shaking event. Generally, a pile supports a superstructure load (Q_{dead}) by mobilizing positive skin friction and tip resistance (Q_{tip}) (Fig. 1a). The positive skin friction is developed by the relative movement of the pile with respect to the surrounding soil. During shaking (i.e., coseismic), excess pore pressures u_e in the soil surrounding the pile can decrease the shaft resistance resulting in the transfer of load to the pile's tip. In turn, the pile tip then carries an increased load while its capacity can also be potentially decreased due to u_e developed around it. Combined, these effects lead to the coseismic settlement of the pile until sufficient resistance is mobilized to balance the load at the tip (Fig. 1b). During reconsolidation, the soil settles relative to the pile and downdrag shear stresses (negative skin friction) at the interface may cause further settlement (Fig. 1b). The depth at which the skin friction changes from positive to negative has been termed the "neutral plane" [1] (Fig. 1b). The location of the neutral plane shown in Fig. 1b is for illustration and should not be considered to be always within the liquefiable layer. It should be noted that the location of the neutral plane is not constant; but is likely to migrate during liquefaction and reconsolidation; depending upon the relative settlement of the soil and the pile. The corresponding axial load distributions in the pile are shown in Fig. 1c. The negative skin friction adds

* Corresponding author.
E-mail addresses: sksinha@civil.iitd.ac.in (S.K. Sinha), kziotopoulou@ucdavis.edu (K. Ziotopoulou), blkutter@ucdavis.edu (B.L. Kutter).

https://doi.org/10.1016/j.soildyn.2024.109020
Received 4 April 2024; Received in revised form 31 August 2024; Accepted 5 October 2024
Available online 20 October 2024

load to the pile, resulting in maximum load (Q_{max}) at the neutral plane (Fig. 1c). The additional load on the pile, developed because of the negative skin friction, is known as drag load ($Q_{drag} = Q_{max} - Q_{dead}$) (Fig. 1c). This causes an increased load potentially causing further settlement (also known as the downdrag settlement) (Fig. 1b). Thus, the total settlement of a pile from a shaking event is comprised of the coseismic settlement and the post-seismic (or post-shaking) downdrag settlement (Fig. 1c). Evaluation of the total settlement, relative settlement, and the maximum axial load on the pile are typically the basis for design. The phenomena affecting the response of axially loaded piles in liquefiable soils have been more extensively summarized and described by Sinha et al. [2] and Sinha et al. [3]. The phenomenon of liquefaction-induced downdrag has also been studied from a broad range of perspectives and approaches by various researchers ([4–8, 8–19]; e [21,22]; to name a few) and Sinha [23] provide an overview thereof.

Existing procedures for designing piles in liquefiable soils do not fully account for the mechanisms that occur during shaking and reconsolidation [3]. This can lead to conservative or unconservative designs. Specifically, the rate and timing of u_e generation/dissipation and soil reconsolidation as well as their effect on the shaft and tip capacities are typically ignored in existing procedures. The state of the practice, e.g., AASHTO [24], uses a force-based approach for designing piles, where the total load acting on the pile is checked against the total resistance with appropriate load and resistance factors. The force-based approach only focuses on internal forces within the pile and ignore its deformation and movement. Whereas, in the displacement-based design approach, the focus is on the actual deformation and movement of the pile. AASHTO [24] recommends a neutral plane method using TzQz analysis to estimate drag loads. The TzQz analysis is a displacement-based method that uses load transfer curves (t-z for the shaft and q-z for the tip) to model the pile's response. The neutral plane method considers the liquefiable layer to be analogous to a consolidating clay layer. As a result, in a TzQz analysis, the load transfer t-z and q-z curves are assumed to be unaffected by u_e changes in the soil surrounding the pile. AASHTO [24] neither provides any method nor recommends calculating the settlement of the pile. Using the force-based method, without accounting for the effect of u_e and evaluating the pile settlement may result in over- or under-designing piles [3]. The findings presented in this paper are also intended to reinforce and strongly advocate the use of displacement-based design procedures using the TzQzLiq analysis, as developed by Sinha et al. [3], by analyzing the response of axially loaded model piles used in hypergravity tests.

Results from several hypergravity tests (e.g., Ref. [25]; Madabhushi et al., 2010; [7,8,19]) have shown that u_e in the soil generated during shaking can significantly decrease the shaft and tip capacity and cause significant settlement of the pile. Sinha et al. [2] observed that the sequencing and pattern of u_e dissipation and soil reconsolidation can affect the development of drag load and downdrag settlement. Finally, in all the above hypergravity tests, most of the pile settlement was observed to be coseismic. The post-seismic settlement was less than 2 % of the pile's diameter despite large drag loads developed.

Enabled and validated against hypergravity model tests, Sinha et al. [26] developed a TzQzLiq analysis methodology for modeling the response of piles in liquefiable soils. This methodology accounted for changes in the pile's shaft and tip capacity as free field u_e developed/dissipated in the soil [35]surrounding the pile. This was achieved by formulating the stiffness and the capacity of the t-z and q-z curves as a function of the excess pore pressure ratio (r_u). Results showed that the TzQzLiq analysis reasonably predicts the time histories of axial load

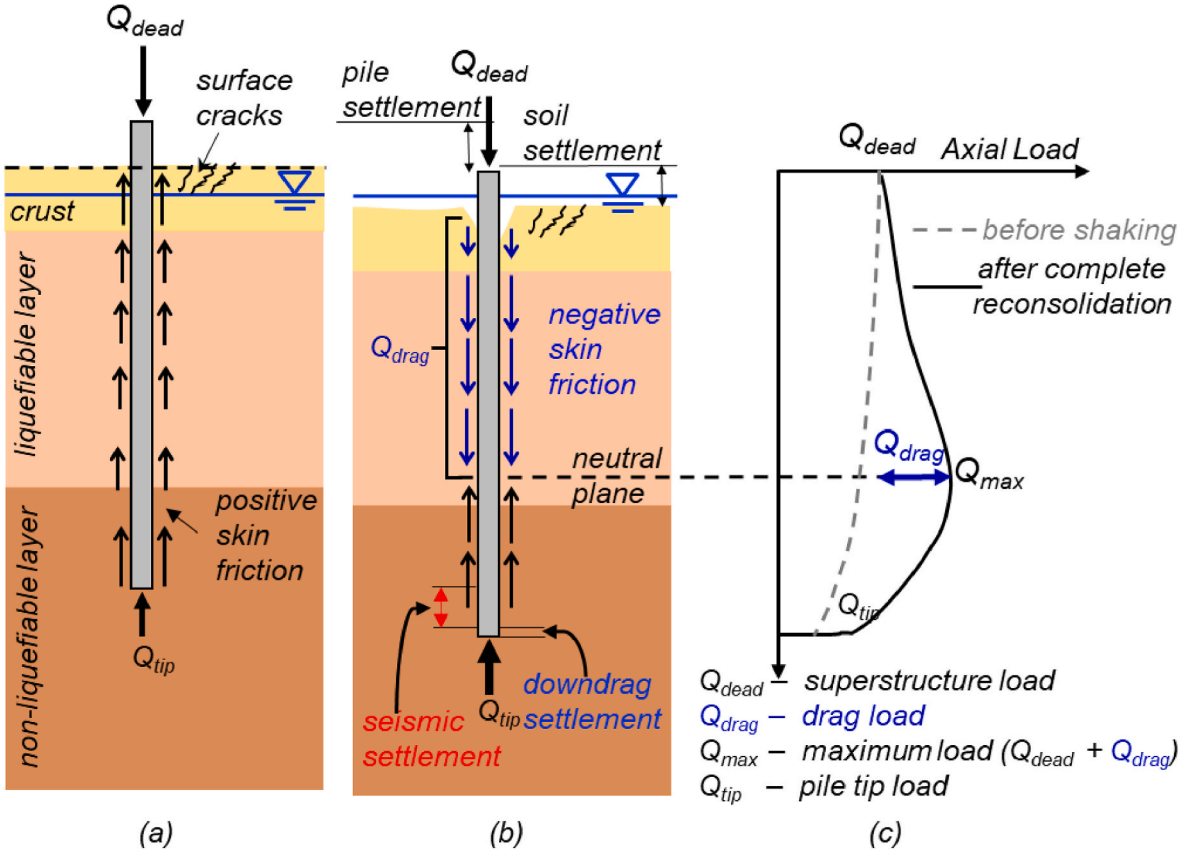

Fig. 1. Schematic illustration of response of axially loaded piles in liquefiable soils: (a) pre-earthquake shaking distribution of pile shaft interface shear stresses and tip load, and (b) during earthquake shaking and reconsolidation: coseismic settlement, development of negative shear stress, soil settlement, downdrag settlement, and neutral plane, and (c) after complete reconsolidation: pile's axial load distribution showing development of drag load and increased load at the tip.

distribution and settlement of axially loaded piles in liquefiable soils both during and post shaking.

This paper presents the deficiencies of the neutral plane method (TzQz analysis) recommended by AASHTO [24] in predicting the drag load as well as the downdrag settlement by comparing them with the TzQzLiq analysis [26] validated with hypergravity model tests. It also studies the u_e changes around the tip and their effect on the pile's response in terms of the axial load distribution and settlement. Results of coseismic settlement, neutral plane depth, downdrag settlement, and drag load are compared such that the pros and cons of the two methods can be clearly established.

2. Description of numerical model

A common method to model the soil–structure interaction is using the Winkler method [27], where the pile is idealized into discrete elements attached to non-linear (t-z and q-z) springs for modeling the load transfer between the soil and the pile [Fig. 2a]. A finite element analysis can be carried out with the pile modeled as a beam element connected with displacement-based load transfer springs (t-z and q-z) with zero-length interface elements to model the pile's response during the shaking event [26]. The load transfer (t-z and q-z) springs model the pile's shaft and tip response, respectively. Depending on whether the load transfer curves account for or ignore the excess pore pressure ratio (r_u) in the soil surrounding the pile, the numerical analysis can be categorized as a TzQzLiq or TzQz analysis, respectively [see Fig. 2b] as described below.

2.1. TzQzLiq analysis: models r_u effect

In the TzQzLiq analysis, the shaft capacity (t_{ult}) and tip capacity (q_{ult}) are each modeled as a function of the excess pore pressure ratio (r_u) around the pile's shaft and near the tip, respectively, as defined in the equations below:

$$\begin{aligned} t_{ult} &= t^{o}_{ult}(1 - r_u) \\ q_{ult} &= q^{o}_{ult}(1 - r_u)^{\alpha_t} \\ \alpha_t &= \frac{3 - \sin\phi'}{3(1 + \sin\phi')} \end{aligned} \tag{1}$$

where t^{o}_{ult} and $q^{o}_{t,ult}$ are the ultimate tip and shaft capacities, respectively, when $r_u = 0$. The impact of the excess pore pressure is naturally a detrimental one. The parameters t^{o}_{ult} and q^{o}_{ult} can be obtained empirically using correlations provided in AASHTO [24] or can be directly measured from pile load tests. The parameter α_t is a constant that, according to Knappett and Madabhushi [25], depends on the effective friction angle (ϕ') of the soil around the tip.

The base and shaft capacity (t_{ult} and q_{ult}) both decrease "during shaking" because of the increased r_u in the soil surrounding the pile (see Equation (1)). Whereas "during reconsolidation", the dissipation of u_e decreases r_u resulting in the regain of the lost shaft and base capacity. After complete reconsolidation (i.e., $r_u = 0$) the shaft and tip capacity become equal to their initial value "before shaking" (i.e., $t_{ult} = t^{o}_{ult}$ and $q_{ult} = q^{o}_{ult}$).

The stiffnesses of the load transfer (t-z and q-z) curves are also scaled proportionally to their respective shaft and tip capacities as defined in Equation 1. [26] describe the selection of the stiffness parameter z_{50} (i.e., the displacement corresponding to mobilization of 50 % of ultimate capacity) for the t-z and q-z material models in OpenSees [28]. The stiffness parameter of the t-z material can be estimated, assuming that a displacement in the order of 3 % of the pile diameter can mobilize the ultimate shaft capacity [26]. The stiffness parameter for the q-z material needs, ideally, to be calibrated from site-specific pile load tests. However, if pile load tests are not available, it is recommended to adopt an empirical pile load test curve or assume that a tip settlement equal to a small fraction of the pile diameter (e.g., 5 % or 10 %) is required to mobilize the ultimate tip capacity [3,26].

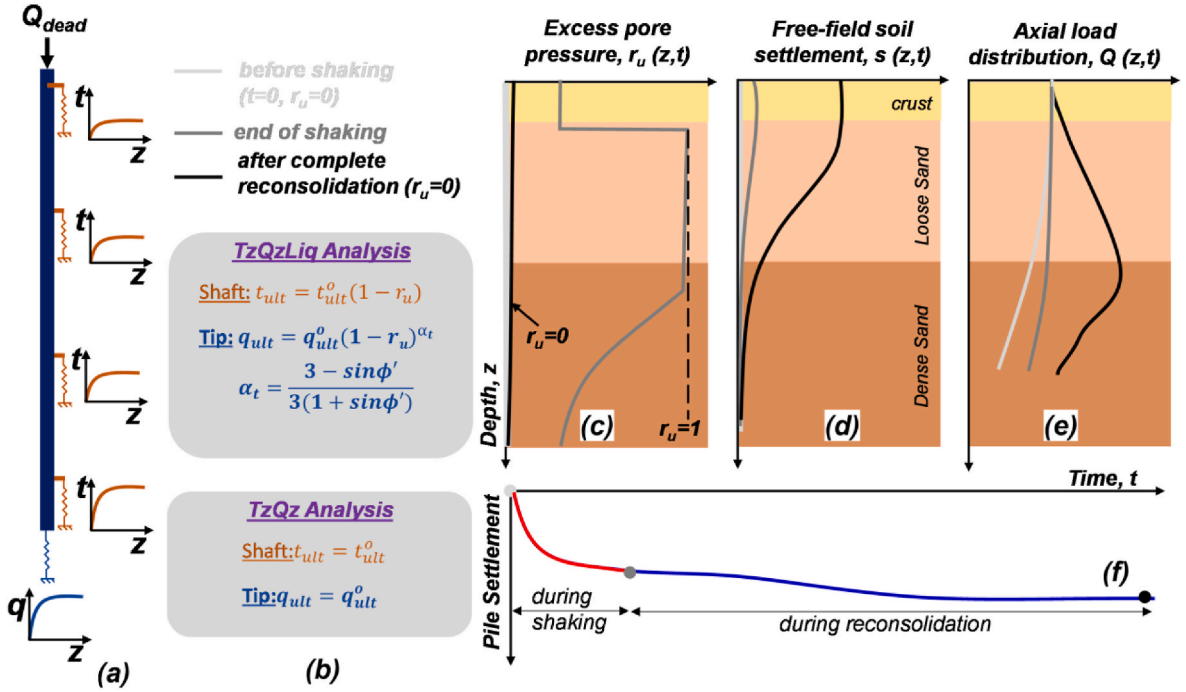

Fig. 2. Conceptual schematic of the approach for simulating the response of axially loaded piles in liquefiable soils with (a) the zero thickness interface elements and load transfer (t-z and q-z) curves using a conventional neutral plane solution method (referred to as TzQz analysis) and a more realistic approach accounting for the effects of excess pore pressures changes on the pile's shaft and tip resistance (referred to as TzQzLiq analysis). Model input parameters include properties of the pile, (b) load transfer (t-z and q-z) curves material properties, (c) isochrones of excess pore pressure ratio (r_u), and (d) soil settlement profiles. Model results include time histories of (e) axial load distribution and (f) pile settlement.

2.2. TzQz analysis: ignores r_u effect

The TzQz analysis can be considered as a special case of the TzQzLiq analysis, where $r_u = 0$. As a result, the shaft and tip capacities remain constant as defined in the equations below:

$$t_{ult} = t^{o}_{ult}$$
$$q_{ult} = q^{o}_{ult} \quad (2)$$

Similarly, the stiffness also remains constant throughout the analysis.

2.3. Analysis procedure

The overall analysis procedure is illustrated in Fig. 2. A dynamic time-history analysis is performed using isochrones of excess pore pressure ratio, $r_u(z,t)$ [Fig. 2c], and soil settlement, $s(z,t)$ [Fig. 2 (d)] profiles to simulate the response of the pile. The results of the model include time histories of axial load distribution [Fig. 2e] and settlement of the pile [Fig. 2f]. The isochrones of $r_u(z,t)$ and $s(z,t)$ can be measured directly from an instrumented model test or can be obtained numerically through a 1-D or 2-D site response analysis.

The analysis is performed in two stages. Stage 1 establishes the initial (at t = 0) axial load distribution with the applied dead loads (Q_{dead}) [Fig. 2e]. It is also quite possible that negative skin friction initially exists in a pile due to post-installation consolidation or from a previous seismic event. In Stage 2, a time-history analysis is performed [Fig. 2] stepping through the isochrones of r_u (z, t) and s (z, t). The time-history analysis performed in Stage 2 predicts settlements, skin friction, and tip loads during the shaking and reconsolidation phase [Fig. 2e]. The results obtained from Stage 2 can be sub-categorized into “during shaking” and “during reconsolidation”. The duration corresponding to the simulated earthquake when u_e develops is referred to as “during shaking” whereas the duration during the dissipation of u_e is referred to as “during reconsolidation”. For example in Fig. 2e, the results obtained from the analysis starting at t = 0 to the end of shaking are referred to as “during shaking" while the results obtained following that are referred to as “during reconsolidation”.

3. Numerical analysis of piles used in hypergravity model tests

Numerical analyses were performed on single piles with embedment depths of 0D, 3D, and 5D in the dense sand layer and with varying pile head loads leading to static factors of safety ranging from 1.6 to 12.4. These piles were tested in hypergravity model tests and were subjected to sequences of shaking events as described below.

3.1. Description of hypergravity model tests

Two series of hypergravity model tests SKS02 [19] and SKS03 [20] were performed on the 9 m-radius centrifuge at the Center for Geotechnical Modeling (CGM) at the University of California Davis at a centrifugal acceleration of 40 g. All the units reported here are in the

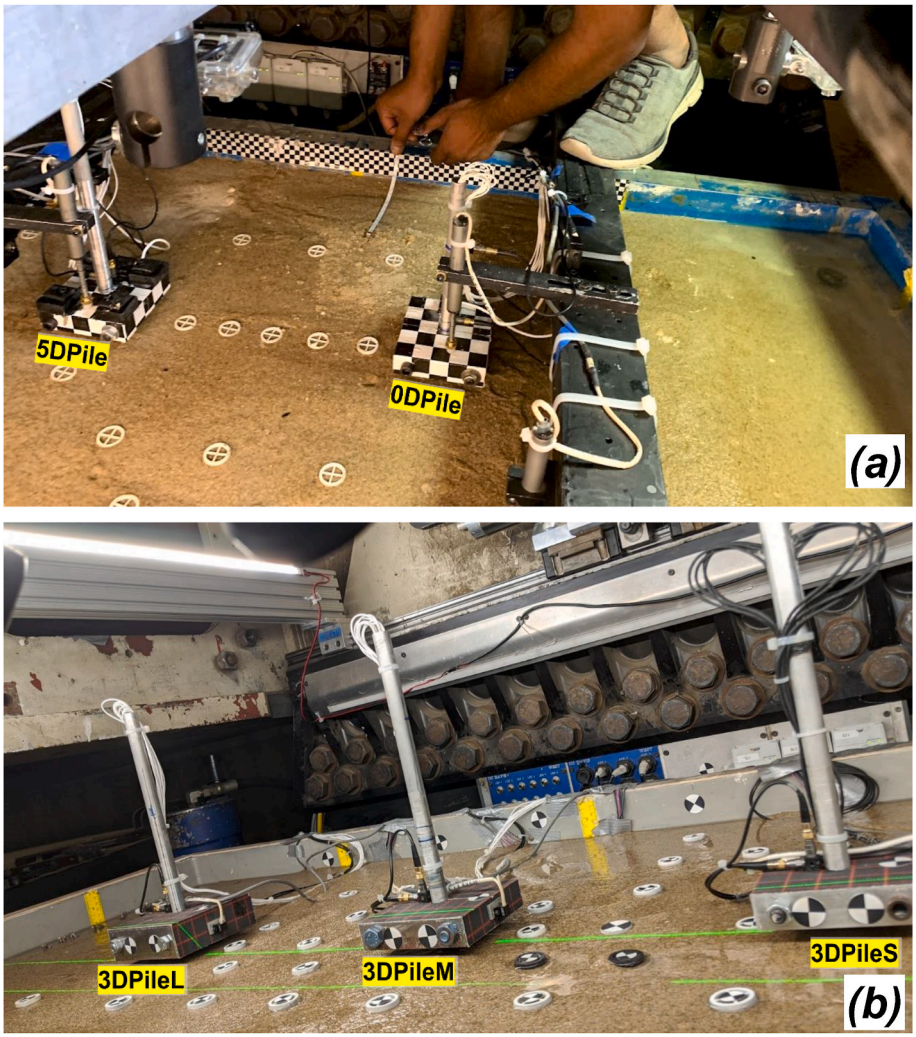

Fig. 3. A view of hypergravity model tests SKS02 [19] and SKS03 [20].

prototype scale following the hypergravity scaling laws by Garnier et al. [29]. A view of hypergravity model tests SKS02 and SKS03 is shown in Fig. 3. The tests modeled 21 m of soil with an undrained rigid boundary condition underneath. Fig. 4 shows the soil profile, the piles, and applied earthquake motions EQM_3 and EQM_4 in the model tests SKS02 and SKS03, respectively.

The model tests SKS02 and SKS03 consisted of uniformly and interbedded layered soil deposits, respectively [Fig. 4a,b]. Table 1 summarizes the layered soil properties. In SKS02, the soil profile included a 1 m-thick Monterey sand layer with relative density (D_R) of 95 %, a 4 m-thick over-consolidated clay layer with an undrained shear strength (s_u) of 20 kPa, a 9 m-thick liquefiable loose sand layer ($D_R \approx 43$ %), and a dense sand layer ($D_R \approx 85$ %) beneath. The SKS03 model had a more complex soil profile, including 1 m of Monterey sand layer, 2 m of clay crust ($s_u \approx 28$–35 kPa), 4.7 m of a loose liquefiable sand layer ($D_R \approx 40$ %), 1.3 m of a clayey silt layer (20 % clay and 80 % silt), 4 m of a medium dense sand layer ($D_R \approx 60$ %), and a dense sand layer ($D_R \approx 83$ %) beneath. The water table was at the ground surface of both models.

The models used densely instrumented aluminum pipe piles with prototype dimensions of outer diameter (D) of 635 mm and a thickness of 35 mm [Fig. 4a,b]. In what follows, the annotations 0D, 3D, and 5D in the name of the piles indicate their embedment depth, i.e., the 3DPile had its tip embedded 3 diameters into the dense sand layer. The SKS02 model featured two piles, 0DPile and 5DPile [Fig. 4a]. Both the 0DPile and 5DPile were loaded with $Q_{dead} = 500$ kN, resulting in a static factor of safety of 5.4 and 12.4, respectively. The SKS03 model consisted of three piles (3DPileS, 3DPileM, and 3DPileL), with all their tips embedded up to 3D in the dense sand layer. The annotations S, M, and L, whenever appearing, correspond to small (500 kN), medium (1500 kN), and large (2400 kN) dead loads applied to the piles. Consequently, the 3DPileS, 3DPileM, and 3DPileL had static factors of safety of 8, 2.6, and 1.6, respectively.

Table 1
Soil layer properties in the two hypergravity model tests SKS02 and SKS03 [8, 19] (Fig. 5).

Hypergravity Model Tests	Layer	Relative Density D_R (%)	Thickness (m)	Saturated Density (kg/m^3)
SKS02	Monterey Sand	95	1	2,054
	Clay	–	2	1,700
	Loose Sand	43	4.7	1,971
	Dense Sand	85	1.3	2,000
SKS03	Monterey Sand	95	1	2,054
	Clay	–	2	1,700
	Loose Sand	40	4.7	1,971
	Clayey Silt	–	1.3	2,000
	Medium-Dense Sand	60	4	1,019
	Dense Sand	86	8	2,051

The models were shaken with multiple scaled Santa Cruz earthquake motions from the Loma Prieta 1989 earthquake of $M_w = 6.9$. Fig. 4 shows the applied shaking motions EQM_3 and EQM_4 and their

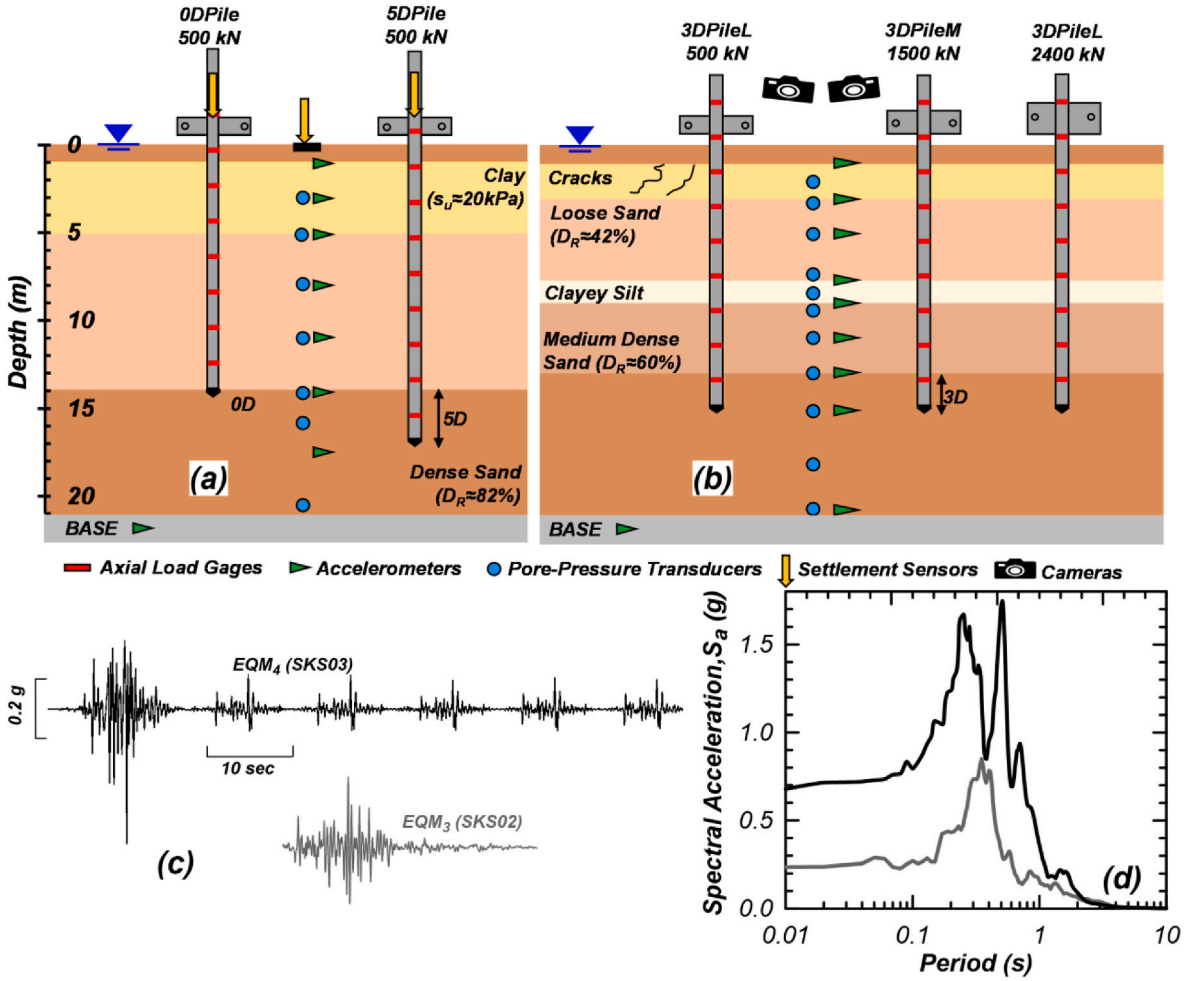

Fig. 4. Cross-sectional view of the hypergravity model tests (a) SKS02 and (b) SKS03; and the (c) applied shaking motions EQM_3 and EQM_4 and their response spectrum.

corresponding acceleration response spectra. Shaking event EQM_3 was the third shaking event in sequence applied to the model SKS02 with a peak base acceleration (PBA) of 0.24 g. Shaking event EQM_4 was the fourth shaking event in sequence applied to the model SKS03. It was a long-duration modified Santa Cruz motion [30] consisting of one large pulse followed by five small pulses, scaled to produce a PBA of 0.45 g. The duration of the shaking was about 30 s.

The models were heavily instrumented with accelerometers, strain gages inside the piles, pore pressure transducers, distributed settlement sensors e.g., line lasers [31], and 3D stereophotogrammetry cameras [32], to measure and track the state of the model during each of the shaking events. The recorded responses of the soil (accelerations, pore pressures, settlements) and piles (accelerations, axial load distribution, settlements) for all shaking events are described in detail by Sinha et al. [19,20]. Fig. 5a,b and Fig. 6a,b show the isochrones of free-field r_u and soil settlement profiles for the shaking events EQM_4 and EQM_3, respectively. Free field r_u profiles were obtained from u_e measured by the pore pressure transducers. The soil settlement profiles were obtained through an inverse analysis of measured u_e profiles constrained by measured surface settlements [26]. Results show that some amount of soil reconsolidation occurs during shaking [Fig. 5b and 6b]. The figures also show the axial load distribution profiles (isochrones) and the time history of pile settlement, of 3DPileS [Fig. 5c,d] for shaking event EQM_4 and 0DPile [Fig. 6c,d] for shaking event EQM_3, respectively. The axial load distribution of the piles was obtained from strain gages attached to the pile [see Fig. 4a,b]. The time history of pile settlement was obtained through the processing of camera images, line laser projections, and measurements from linear variable differential transformers (LVDTs) ([8,19,31–33] e). The axial load distribution and settlement of the rest of the piles during the selected shaking events are described in detail by Sinha [23].

Hypergravity pile load tests were conducted at the beginning as well as at the end of shaking events to determine the shaft and tip capacity of the piles. Sinha et al. [2] describe the pile load tests and their

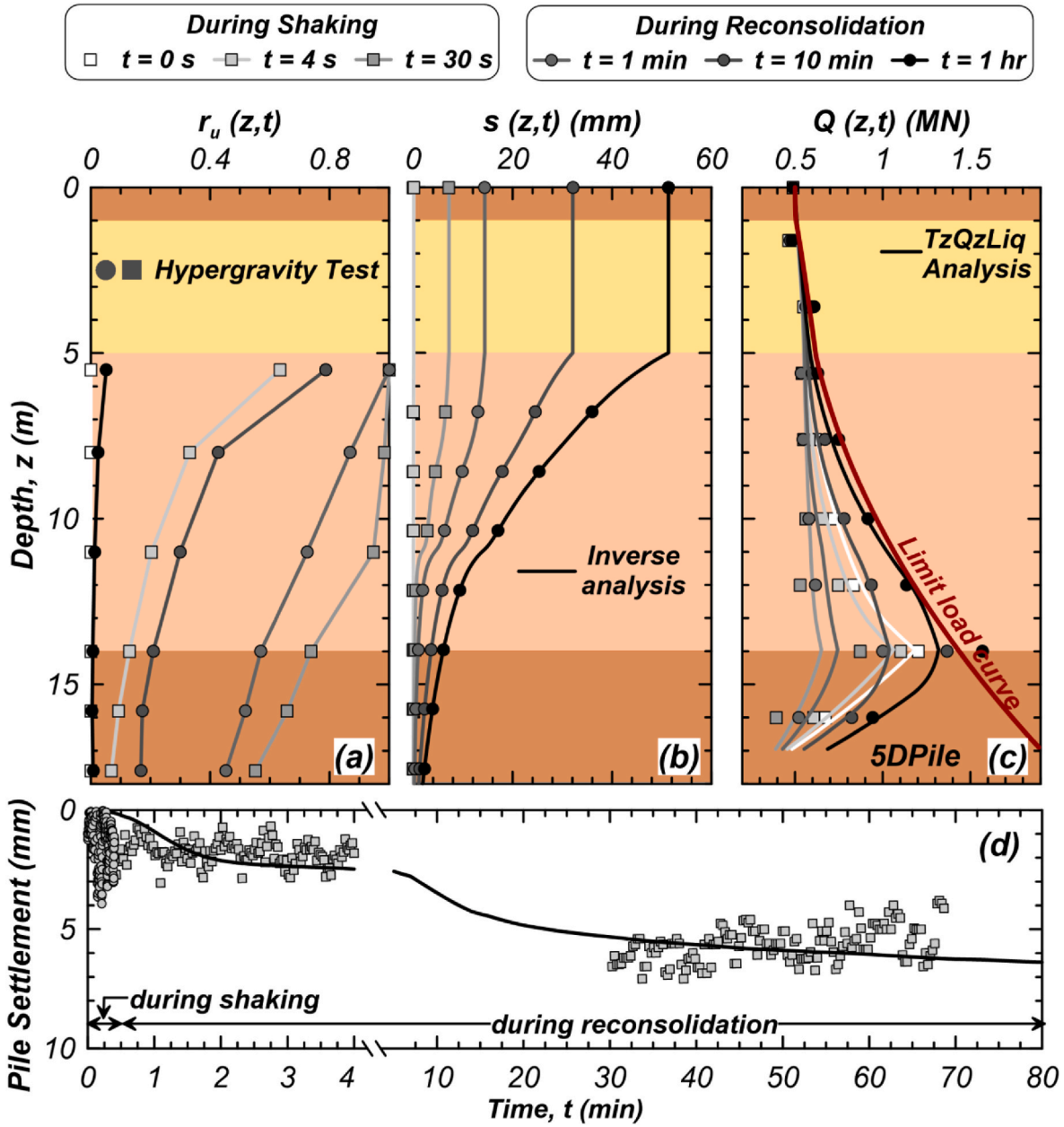

Fig. 5. Validation of TzQzLiq analysis of 5DPile for shaking event EQM_3 in hypergravity test SKS02: Isochrones of (a) effective stress; (b) soil settlement; (c) axial load distribution profiles at selected times during and reconsolidation; and (d) complete time history of pile settlement.

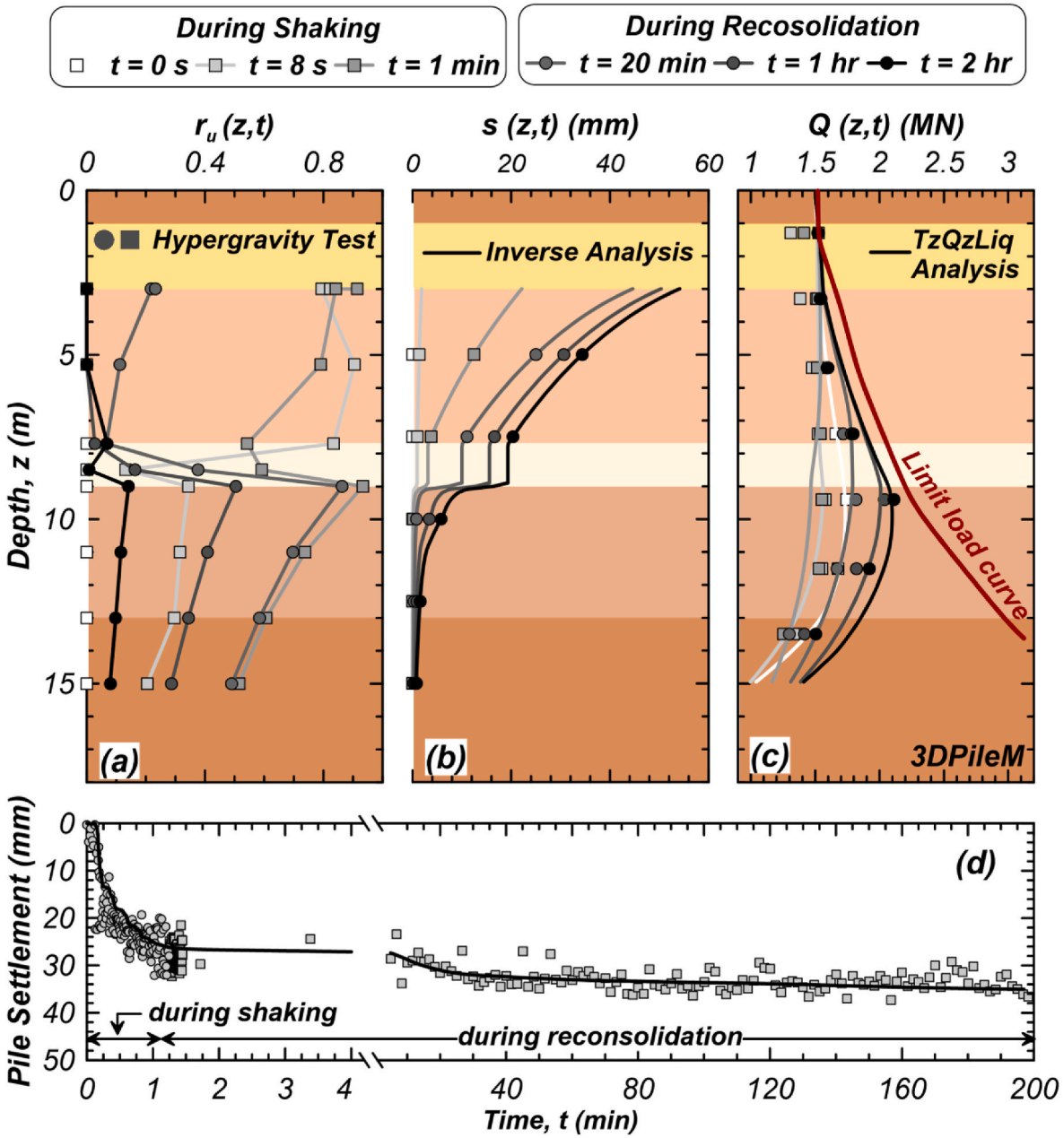

Fig. 6. Validation of TzQzLiq analysis of 3DPileM for shaking event EQM_4 in hypergravity test SKS03: Isochrones of (a) effective stress; (b) soil settlement; (c) axial load distribution profiles at selected times during and reconsolidation; and (d) complete time history of pile settlement.

interpretation for obtaining the shaft and tip capacities of the piles. The limit load curves for the piles, which are defined as the axial load distribution assuming maximum drag load development [2], used in model tests SKS02 and SKS03, are shown in Fig. 5c and 6c, respectively. The limit load curve is obtained from the summation of the pile head load and the cumulative integration of the pile's interface shear strength with depth, assuming the pile mobilizes negative skin friction equal to its interface shear strength.

3.2. Numerical analysis

The numerical analysis was performed in OpenSees [28] with a mesh discretization of 0.1 m long elements. Displacement-based load transfer t-z and q-z springs with zero-length elements were used to model the pile's response. The materials used for the interfaces t-z and q-z were the TzLiq [34] and QzLiq [26] material models, respectively. The functional dependence and behavior of the backbone curves for the TzLiq and QzLiq material is similar to the p-y material described by Boulanger et al. [34]. The load-path of the TzLiq and QzLiq as an effect of excess pore pressure is provided in the examples of OpenSees documentation (https://opensees.github.io/OpenSeesDocumentation) and also included in Boulanger et al. [34] and Sinha et al. [26]. Table 2 summarizes the interface material properties used in the analysis, which were validated through the result of the hypergravity pile load test [26]. The TzLiq and QzLiq materials implemented in OpenSees [28] can model both types of interface behavior: one considering the effect of r_u (referred to as TzQzLiq analysis) and the other ignoring r_u (referred to as TzQz analysis). The material model has a parameter "updateMaterialStage" that can be used to switch between the TzQz (updateMaterialStage = 0) and TzQzLiq (updateMaterialStage = 1) analysis [26].

The complete analysis was performed in two stages. Stage 1 established the initial (at t = 0) axial load distribution with the applied dead

Table 2
Material properties used in the numerical (TzQzLiq and TzQz) analyses of 0DPile and 5DPile for shaking event EQM_3 in hypergravity model test SKS02, and the 3DPiles (3DPileS, 3DPileM, and 3DPileL) for shaking event EQM_4 in hypergravity model test SKS03.

Soil Layers	t-z Properties		Piles	q-z Properties	
	z_{50} (% D)	t^o_{ult} (kN)		z_{50} (% D)	q^o_{ult} (kN)
Clay and Silt Layers	0.31	Limit load curve[a]	0DPile	7	2,745
Loose, Medium Dense Sand	0.31		5DPile	7	7,137
Dense Sand	0.15		3DPiles	9	4,576

[a] for 0DPile and 5DPile is shown in Fig. 4, and for 3DPiles is shown in Fig. 5.

loads (Q_{dead}) (Fig. 5c and 6c). For the selected shaking events EQM_3 and EQM_4, the piles had an initial drag load. As a result, many iterations were performed to determine the required soil settlement profile that could result in the shear stress development leading to the initial axial load distribution. Fig. 5c and 6c show a very good agreement of the initial axial load distribution (i.e., at t = 0) obtained from the numerical analysis with the hypergravity tests. Stage 2 performed a dynamic time history analysis by stepping through the isochrones of r_u (z, t) and s (z, t) profiles.

3.3. Validation

The numerical analysis procedure was validated with dynamic TzQzliq analyses performed on a selected pile for each of the hypergravity model tests, i.e., 5DPile from the model test SKS02 and 3DPileS from the model test SKS03. The comparison of the isochrones of axial load distribution Q (z, t) and time history of pile settlement for 5DPile (for shaking events EQM_3) and 3DPile (for shaking event EQM_4) obtained from the TzQzLiq analysis with hypergravity test results are shown in Fig. 5c,d and Fig. 6c,d, respectively. Table 3 compares the pile settlement and drag load obtained from the TzQzLiq analysis with the hypergravity test. During shaking, the u_e in the liquefiable (and later liquefied) layer reduced the negative skin friction, decreasing the drag loads, and ultimately diminishing it to zero at full liquefaction ($r_u \approx 1$) [Fig. 5b,c and Fig. 6b,c]. However, as pore pressures later on dissipated, the drag loads again increased, approaching or surpassing the drag load that existed before shaking [Fig. 5c and 6c]. During shaking, while drag loads decreased, the loss of the shaft friction and especially the tip capacity (with now more load transferred to the pile's tip), resulted in a significant settlement of the piles [Fig. 5d and 6d]. For 3DPileL, the loss of tip capacity was so much that the pile plunged into the soil (i.e., suffered coseismic settlement of >10 % D) [Table 3]. During reconsolidation, while large drag loads developed, the resulting settlement was small (<2 % D) [Table 3]. It should be noted that the hypergravity model tests used for validation cover a wide range of piles i.e., lightly to heavily loaded piles with their tip embedded shallow as well as deep in the dense sand layer [see Table 3]. Similarly, the consequences from the liquefaction of the soil in terms of pile settlement cover a wide range: small settlements (in the cases of the 3DPileS and 0DPile) to plunging of pile (in case of 3DPileL). It can be observed in Fig. 5c and 6c that the axial load distribution of the pile (during shaking and reconsolidation) obtained through the TzQzLiq analysis reasonably matched the hypergravity test results. Similarly, the time history of pile settlement was in good agreement with the hypergravity test results [Fig. 5d and 6d]. It can also be observed from Table 3 that the results from the TzQzLiq analysis show very good agreement on the pile settlement (coseismic, downdrag, and total) and drag load with hypergravity tests for all the 5 piles (0DPile, 5DPile, 3DPileS, 3DPileM, and 3DPileL) modeled. Overall, the results from the numerical analysis matched quite well with the hypergravity test, thus validating the TzQzLiq analysis in capturing the complete response of axially loaded piles in liquefiable soils during a shaking event.

Table 3
Comparison of pile settlement and drag load results obtained from the TzQzLiq analyses of 0DPile, 5DPile, and the 3DPiles (3DPileS, 3DPileM, and 3DPileL) for shaking event EQM_3 in model test SKS02 and shaking event EQM_4 in model test SKS03 respectively, against the measurements recorded in the hypergravity tests.

Pile	Methods	Pile Settlement (%D)			Drag Load (kN)
		Coseismic	Downdrag	Total	
0DPile	Hypergravity Test	1.7 %	1.4 %	3.10 %	498
	TzQzLiq Analysis[a]	1.3 %	1.7 %	3.00 %	440
	TzQz Analysis[b]	–	1.9 %	1.90 %	550
5DPile	Hypergravity Test	0.0 %	0.8 %	0.80 %	1,068
	TzQzLiq Analysis[a]	0.0 %	0.9 %	0.90 %	850
	TzQz Analysis[b]	–	0.9 %	0.90 %	1080
3DPileS	Hypergravity Test	0.3 %	0.6 %	0.90 %	600
	TzQzLiq Analysis[a]	0.4 %	0.8 %	1.20 %	700
	TzQz Analysis[b]	–	0.8 %	0.80 %	800
3DPileM	Hypergravity Test	4.4 %	0.9 %	5.30 %	620
	TzQzLiq Analysis[a]	4.4 %	1.1 %	5.50 %	600
	TzQz Analysis[b]	–	0.9 %	0.90 %	750
3DPileL	Hypergravity Test	31.5 %	1.1 %	32.60 %	–
	TzQzLiq Analysis[a]	19.3 %	1.2 %	20.50 %	686
	TzQz Analysis[b]	–	2.5 %	2.50 %	640

[a] Effect of the change in r_u in the soil surrounding the pile is accounted for in the pile's interface load-transfer curves.
[b] Changes in r_u around the pile are not accounted for in the pile's interface load-transfer curves.

4. Comparison of TzQzLiq and TzQz analysis

TzQzLiq and TzQz analyses were performed on piles (0DPile, 5DPile, 3DPileS, 3DpileM, and 3DPileL) for the selected shaking events, and their results on load transfer curves, drag load, pile settlement, and the neutral plane were compared. Both types of analysis used the same input parameters for the t-z and q-z material properties [Table 2], free-field r_u (z,t), and soil settlement s (z,t) profiles [Fig. 5c,d and Fig. 6c,d]. The only difference between the TzQzLiq and the TzQz analysis was setting the state of the "updateMaterialStage" parameter for the interface materials. In the TzQzLiq analysis, the "updateMaterialStage" was set to 1 whereas for the TzQz analysis, it was set to 0. The subsections below compare the response of the pile obtained from the TzQzLiq analysis with the TzQz analysis. Fig. 7 compares the load-displacement response of the pile's interface. Figs. 8–12 compare the pile axial load distribution before shaking and after complete reconsolidation, pile settlement, drag load, depth of the neutral plane, and load-displacement behavior of the pile's tip. It should be noted that since the TzQz analysis does not account for r_u changes in the soil, the pile's response is only affected by the soil settlement that occurs from the shaking event. As a result, for the TzQz analysis, the response is not categorized into coseismic and post-shaking downdrag settlement as it is done for the TzQzLiq analysis [see Fig. 8b,c,d,e to Fig. 12b,c,d,e]. Table 3 summarizes the pile settlement and the drag load obtained from the hypergravity tests and compares it with the TzQzLiq and TzQz analysis.

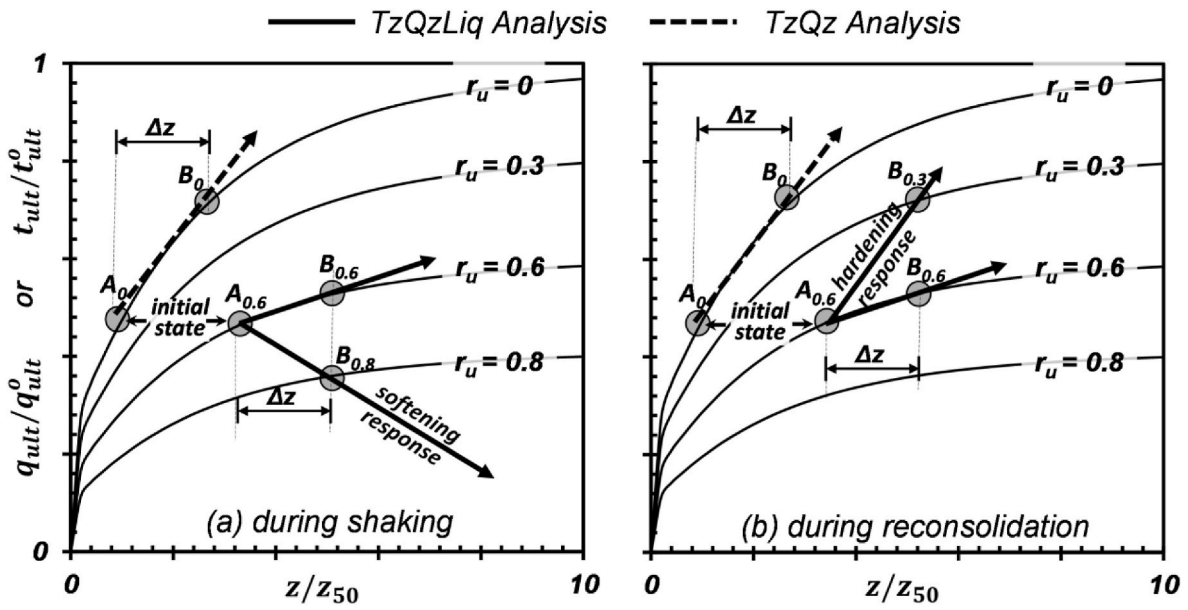

Fig. 7. Illustration of the comparison in the mechanism of pile's (shaft and tip) load-displacement response $A_x \rightarrow B_x$ (for a given displacement (Δz)) from an initial state A_0 in the TzQzLiq (where the effect of r_u is considered and $r_u = 0.6$) with the initial state A_0 from the TzQz (where the effect of r_u is neglected i.e., $r_u = 0$) analysis. (a) During shaking, the increase in r_u results in a softening response in the TzQzLiq analysis leading to more settlement than in the TzQz analysis. (b) During reconsolidation, the decrease in r_u results in a hardening response in the TzQzLiq analysis which can mobilize even larger resistance compared to the TzQz analysis considering the rate of reconsolidation (i.e., Δr_u) is high.

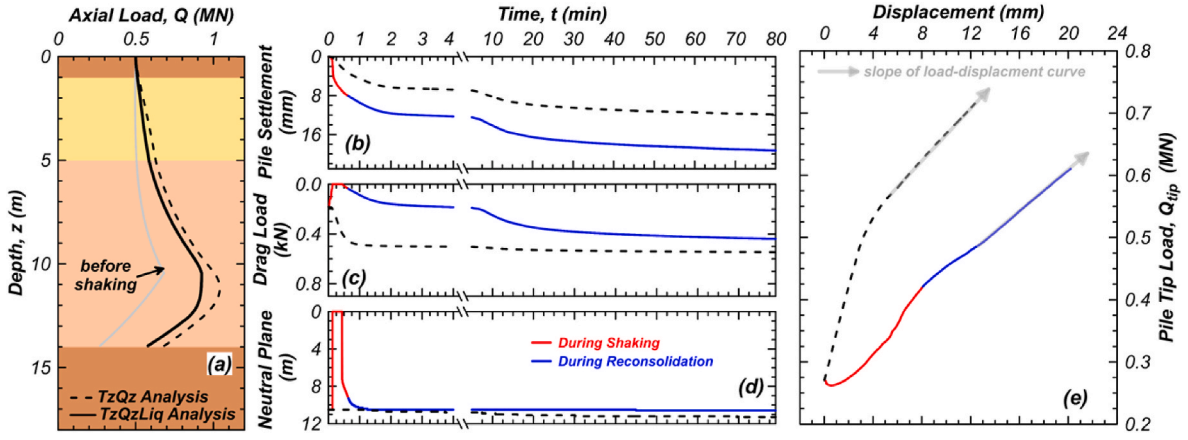

Fig. 8. Comparison of results from TzQzLiq with TzQz analysis for 0DPile for shaking event EQM_3 in the hypergravity model test SKS02: (a) initial and final (after complete reconsolidation) axial load distribution profiles; time histories of (b) pile settlement, (c) drag load, (d) neutral plane depth; and (e) load-displacement response of pile's tip.

4.1. Load-displacement response

The response of the pile depends on the interface behavior i.e., the load transfer t-z and q-z curves. The pile's skin friction and tip resistance are mobilized through the settlement of its tip. During a shaking event, the pile always undergoes settlement, either due to the seismic load and the increase in u_e, or the development of drag load. Depending on the rate of excess pore pressure generation/dissipation and the initial position on the load curve, the interface can have a normal, softening, or hardening response compared to the case when the effects of r_u are neglected. Fig. 7 shows an illustration of the comparison of the interface load-displacement response during a shaking event obtained from TzQzLiq analysis with TzQz analysis. Fig. 7 also shows the decrease in capacity and stiffness of load transfer curves with increasing r_u. In the illustration, a given displacement (Δz) is applied to the initial state of the interface, which is assumed at $A_{0.6}$ (with $r_u = 0.6$) in the TzQzLiq analysis and A_o (with $r_u = 0$) in the TzQz analysis [Fig. 7]. Please note that both of the initial states $A_{0.6}$ and A_o represent the same load but have different initial displacements (and hence stiffness) because of the different load-transfer curves [Fig. 7].

During shaking, the development of u_e can significantly decrease the pile's tip capacity and stiffness resulting in large settlements. Fig. 7a compares the response from the TzQzLiq with the TzQz analysis. In the TzQz analysis, since changes in r_u are not accounted for, the response path will be $A_0 \rightarrow B_0$. On the other hand, in the TzQzLiq analysis, depending on the changes in r_u, the response path can either have a normal behavior $A_{0.6} \rightarrow B_{0.6}$ (assuming no change in r_u) or a softening behavior $A_{0.6} \rightarrow B_{0.8}$ (assuming r_u increased from 0.6 to 0.8). It can be observed that for both of the paths ($A_{0.6} \rightarrow B_{0.6}$, $A_{0.6} \rightarrow B_{0.8}$) since the stiffness and mobilized capacity are much lower than the load curve with $r_u = 0$, the pile undergoes significant settlement in the TzQzLiq analysis as compared to the TzQz analysis. Furthermore, it is also observed that since the increase of r_u results in a softening behavior, it results in causing even more settlement of the pile. Fig. 8b compared to

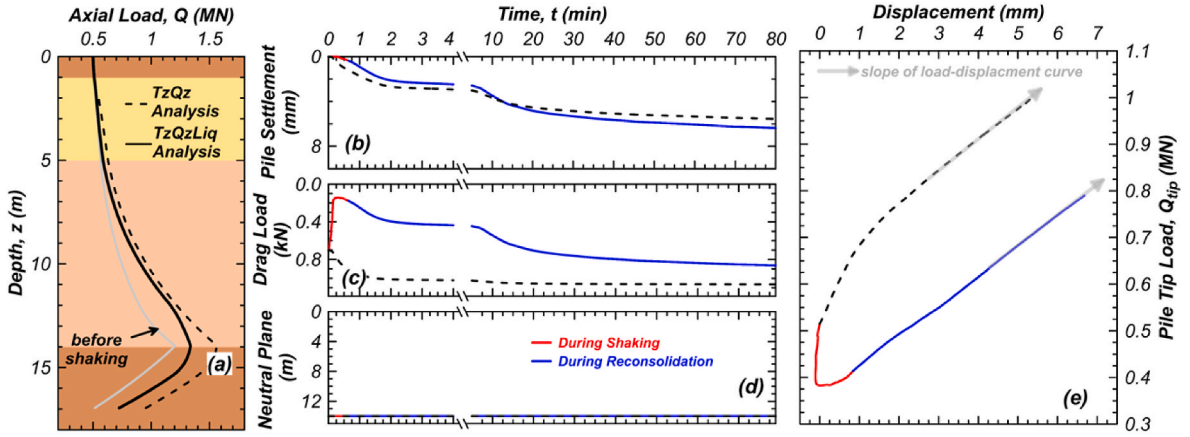

Fig. 9. Comparison of results from TzQzLiq with TzQz analysis for 5DPile for shaking event EQM_3 in the hypergravity model test SKS02: (a) initial and final (after complete reconsolidation) axial load distribution profiles; time histories of (b) pile settlement, (c) drag load, (d) neutral plane depth; and (e) load-displacement response of pile's tip.

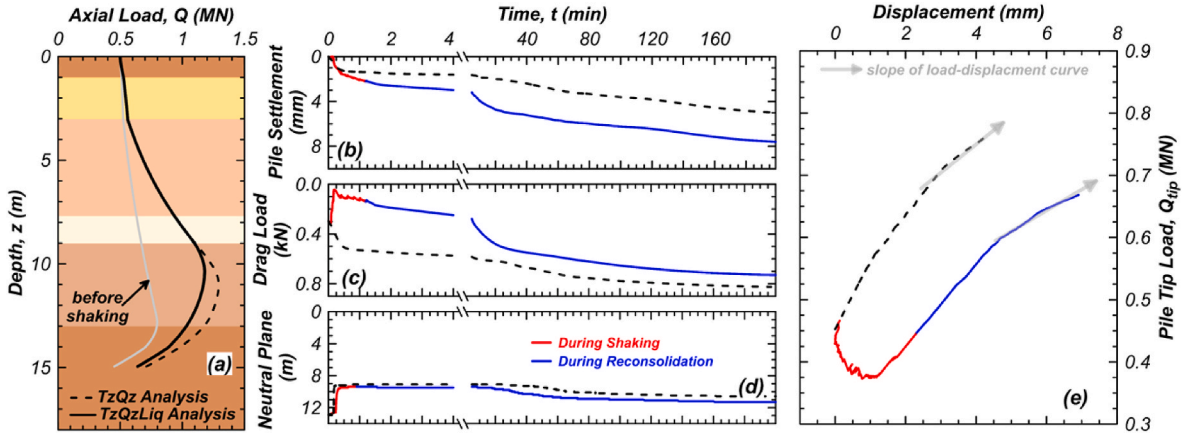

Fig. 10. Comparison of results from TzQzLiq with TzQz analysis for 3DPileS for shaking event EQM_4 in the hypergravity model test SKS03: (a) initial and final (after complete reconsolidation) axial load distribution profiles; time histories of (b) pile settlement, (c) drag load, (d) neutral plane depth; and (e) load-displacement response of pile's tip.

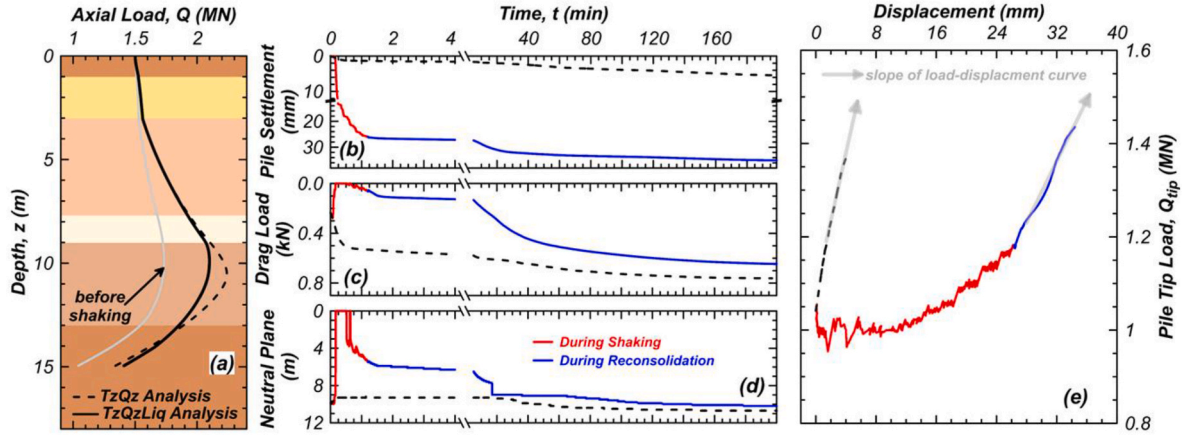

Fig. 11. Comparison of results from TzQzLiq with TzQz analysis for 3DPileM for shaking event EQM_4 in hypergravity model test SKS03: (a) initial and final (after complete reconsolidation) axial load distribution profiles; time histories of (b) pile settlement, (c) drag load, (d) neutral plane depth; and (e) load-displacement response of pile's tip.

Fig. 12d shows that the pile, during shaking, can undergo significant settlement due to the effect of increased r_u around it. Fig. 13 shows that with the increase in r_u at the pile's tip, the settlement of the pile increases. For very high r_u, the settlements approached values equal to the full diameter of the pile.

During reconsolidation, the soil settlement increased the drag load,

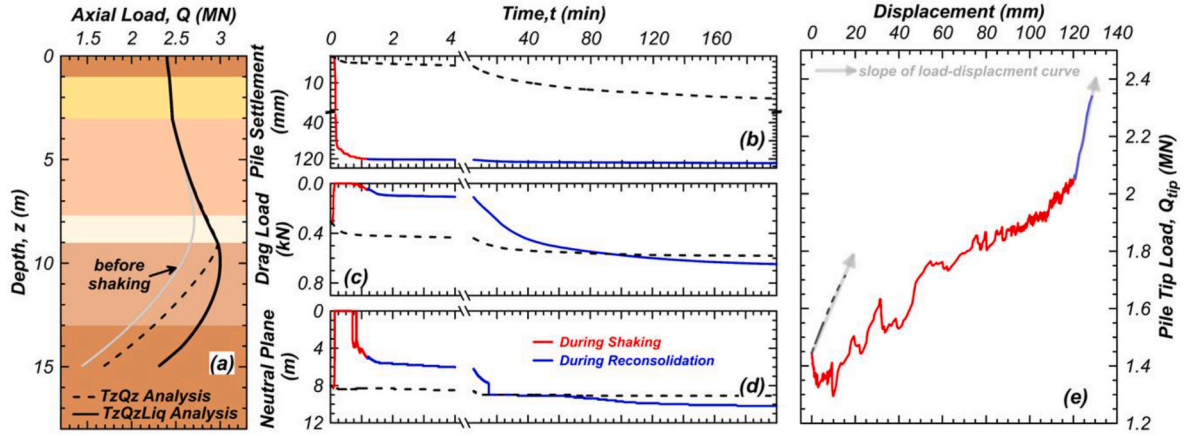

Fig. 12. Comparison of results from TzQzLiq with TzQz analysis for 3DPileL for shaking event EQM_4 in the hypergravity model test SKS03: (a) initial and final (after complete reconsolidation) axial load distribution profiles; time histories of (b) pile settlement, (c) drag load, (d) neutral plane depth; and (e) load-displacement response of pile's tip.

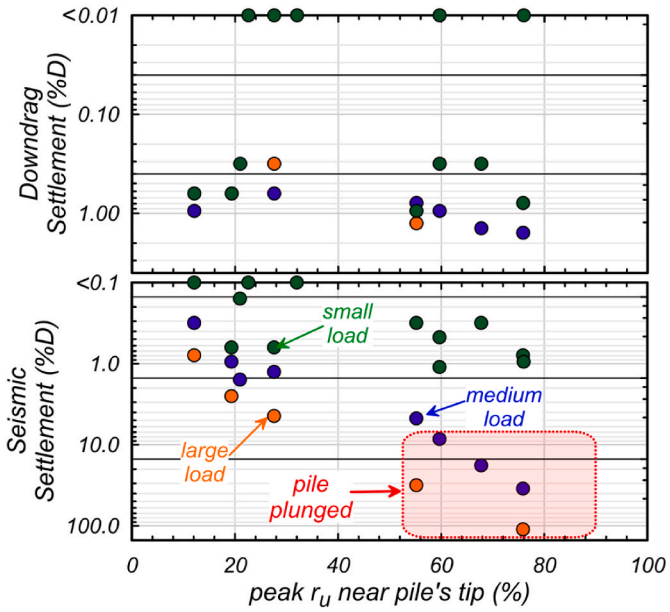

Fig. 13. Summary of coseismic and downdrag settlement of the piles (with small, medium, and large loads with the static factor of safety (FS) > 5, 2.5 < FS < 5, and FS < 2.5, respectively) used in hypergravity model tests SKS02 and SKS03 as a function of the peak excess pore pressure ratio (r_u) near the pile's tip. (data from Sinha [23]).

while at the same time the decrease in u_e increased the pile's tip capacity and stiffness. The magnitude of pile settlement would thus depend on the rate of decrease in r_u and the mobilized load. Fig. 7b compares the response from the TzQzLiq with the TzQz analysis. In the TzQz analysis, the response path will be $A_0 \rightarrow B_0$. On the other hand, in the TzQzLiq analysis, depending on the changes in r_u, the response path can either have a normal behavior $A_{0.6} \rightarrow B_{0.6}$ (assuming no change in r_u) or a hardening behavior $A_{0.6} \rightarrow B_0$ (assuming r_u decreased from 0.6 to 0). It can be observed that for a slower u_e dissipation (for example, the path $A_{0.6} \rightarrow B_{0.6}$), the increase in stiffness and mobilized capacity in the TzQzLiq analysis would still be lower than the TzQz analysis and thus would result in a comparatively larger downdrag settlement (and correspondingly smaller drag load). On the other hand, for a faster rate of u_e dissipation (i.e., the path of $A_{0.6} \rightarrow B_0$), the increase in stiffness and mobilized capacity can be much higher than the one with the load curve with $r_u = 0$, resulting in a smaller settlement (and correspondingly larger drag load) in the TzQzLiq analysis than the TzQz analysis. Table 3 shows that for most cases the downdrag settlement for both types of analysis is similar. However, due to the lowering of stiffness as an effect of r_u, the drag load is smaller in the TzQzLiq analysis compared to the TzQz analysis. As can be observed in Fig. 8e–11e, the slope of the pile's tip load-displacement curve during reconsolidation is steeper for the TzQz analysis than the TzQzLiq analysis. In contrast to the common observation, for the case of the heavily loaded 3DPileL [Table 3], a larger downdrag settlement (correspondingly smaller drag load) is observed in the TzQz analysis compared to the TzQzLiq analysis. This can be again explained through the steeper slope of the 3DPileL's tip load-displacement curve for the TzQzLiq analysis than the TzQz analysis [Fig. 12e].

4.2. Drag load

In the TzQzLiq analysis, the drag load first decreased and then increased. During shaking, the increase in u_e caused a decrease in drag load and a shallower neutral plane [Fig. 8c,d to Fig. 12c,d]. During reconsolidation, as u_e dissipated and the soil settled, the drag load increased again, and the neutral plane deepened [Fig. 8c,d to Fig. 12c, d]. The heavily loaded piles (3DPileM and 3DPileL) and shallowly embedded piles (0DPile) experienced a complete reduction in drag load, causing the neutral plane to reach the ground surface. In contrast, the changes in neutral plane depth for 5DPile and 3DPileS were minimal. Shortly after shaking (within a few minutes, approximately 2–3 min), the neutral plane returned close to its initial depth before shaking, with only a slight increase in drag load. The observed soil settlement during reconsolidation, about 10–20 mm, indicates that even a small amount of soil settlement is sufficient to restore the neutral plane to its pre-shaking depth [Fig. 8d–12d].

In the TzQz analysis, the soil settlement during shaking and reconsolidation caused an increase in the drag loads throughout the shaking event [Fig. 8c–12c]. Similarly, the neutral plane depth also increased throughout the shaking event. However, for cases where the pile had a deeper initial neutral plane and the negative skin friction was not fully mobilized (such as 3DPileS and 3DPileM), the initial soil settlement during shaking first caused a decrease in the neutral plane depth [see Fig. 10d and 11d]. For both the TzQzLiq and TzQz analyses, the final drag load (i.e., after complete reconsolidation) was higher than the initial drag load. The piles with a deep embedment and light loads resulted in larger drag loads and a deeper neutral plane depth compared to heavily loaded piles.

The drag load predicted by the TzQz analysis was generally higher than that predicted by the TzQzLiq analysis, especially for the piles with

small and medium pile head loads (i.e., 3DPileS, 3DPileM, 0DPile, 5DPile) [see Table 3]. The magnitude of the final drag load depends on the stiffness of the pile's tip response during the reconsolidation phase. The reason for the smaller drag load in the TzQzLiq analysis compared to the TzQz analysis is the lower stiffness of the pile's tip accounting for the effect of r_u in soil [Fig. 8a,c,e to Fig. 11b,c,e]. However, for heavily loaded piles, where the initial mobilized tip load is already close to its capacity (resulting in a smaller tip stiffness), the hardening arising from the dissipation of r_u can result in a much stiffer tip response (compared to the TzQz analysis), overall leading to the development of large drag loads [see Table 3]. This is observed in the case of 3DPileL [Fig. 12b,c,e], where the TzQzLiq analysis resulted in larger drag loads than the TzQz analysis. Since the piles are generally designed with a factor of safety of 2 or higher, the results demonstrate that the prediction of drag load from the neutral plane method (i.e., in the TzQz analysis) is overly conservative. For such cases where large drag loads are a concern, the piles are usually designed to be longer for their additional resistance and stability, however, this increases the project's operational challenges and the associated cost.

4.3. Pile settlement

The coseismic settlement was only predicted by the TzQzLiq analysis. Results show that for the cases where the pile settlements were larger, coseismic settlement had the largest contribution [Table 3, Fig. 13]. While the drag loads decreased during shaking, the decrease in the pile's tip capacity and stiffness was so profound that it caused significant settlement of piles [Fig. 8b,c,e to Fig. 12b,c,e]. The piles that had smaller static factors of safety (3DPileM and 3DPileL) suffered significant coseismic settlements. 3DPileL, which had a static factor of safety of 1.6 plunged in the soil (i.e. coseismic settlement >20%D) [Fig. 12]. Sinha [33] observed an increase in coseismic settlement as the r_u near the pile's tip increased [Fig. 13]. Piles loaded with smaller head loads (3DPileS and 0DPile) or deeper embedments (5DPile) suffered smaller coseismic settlements [Table 3, Fig. 13].

The downdrag settlement was predicted by both the TzQzLiq and TzQz analyses, and its magnitude was found to be very similar [Table 3]. The rate of downdrag settlement is observed to be non-linear with time, similar to soil reconsolidation. It is significantly faster at the beginning and then decreases as the soil fully reconsolidates. Although large drag loads developed, the resulting downdrag settlement was limited to <2 % D [Table 3, Fig. 13].

5. Conclusions

This paper compared the results of a TzQzLiq analysis with the neutral plane method ignoring the effect of excess pore pressures (referred to as TzQz analysis) and presented its implication on pile design. The results presented were for single piles where axial behavior governs the pile design. The TzQzLiq analysis was shown to accurately model the response of axially loaded piles in liquefiable soils in hypergravity model tests. The hypergravity model tests used for validation covered a wide range of piles i.e., lightly to heavily loaded piles with their tip embedded shallow as well as deep in the dense sand layer. Results of pile settlement (including coseismic and downdrag) and drag load from the TzQzLiq analysis matched quite well with the model tests. On the other hand, the neutral plane analysis could only predict downdrag settlement and drag load. Analysis results clearly showed that while the neutral plane analysis predicts a similar downdrag settlement (compared to the TzQzLiq analysis), it usually overpredicts drag loads. Since the current state of practice (such as AASHTO [24]), uses a force-based design, the overpredicted drag loads may result in longer design lengths of piles, ultimately leading to increased project costs and operational challenges.

Pile settlement and drag load development are primarily influenced by the behavior at the pile tip. During shaking, the generation of excess pore pressures at the pile tip leads to a softening response, resulting in significant coseismic settlement. As a result, the most substantial pile settlement occurred during shaking. During reconsolidation, the rate of the excess pore pressure dissipation and the initial load on the pile influenced drag load development. For lightly and moderately loaded piles (with a static factor of safety >2.5), the overall tip stiffness in the TzQzLiq analysis was lower than in the TzQz analysis, leading to smaller drag loads. In contrast, for heavily loaded piles (where the mobilized tip load was much farther along the load curve resulting in lower stiffness), the hardening effect from excess pore pressure dissipation caused a much stiffer response in the TzQzLiq analysis compared to the TzQz analysis, ultimately resulting in larger drag loads. Although reconsolidation-induced soil settlement generated significant drag loads, the resulting downdrag settlement remained minimal, typically less than 2 % of the pile diameter.

A displacement-based approach that evaluates pile performance (i.e., the pile settlement and the maximum load) and accounts for all the mechanisms observed during a shaking event, should be used for designing piles in liquefiable deposits. Relying solely on a force-based design approach, which neglects pile settlement, may lead to under- or over-design, resulting in either unsafe or uneconomical outcomes. The findings in this paper support the need for a displacement-based design procedure using the TzQzLiq analysis. Sinha et al. [3] introduced a simplified TzQzLiq analysis to establish a displacement-based design procedure for axially loaded piles in liquefiable soils. The procedure offers a design curve relating pile settlement and maximum load across varying pile lengths, enabling designers to select an appropriate pile length depending based on the serviceability criteria and structural strength requirements.

The hypergravity test data used in this study are made available through the DesignSafe project PRJ-2828 [19,20].

CRediT authorship contribution statement

Sumeet K. Sinha: Conceptualization, Methodology, Visualization, Validation, Software, Resources, Investigation, Formal analysis, Data curation, Writing - Original Draft. **Katerina Ziotopoulou:** Conceptualization, Methodology, Writing - Review & Editing, Supervision, Project administration, Funding acquisition. **Bruce L. Kutter:** Conceptualization, Methodology, Writing - Review & Editing, Supervision, Funding acquisition.

Declaration of competing interest

The authors declare that they have no known competing financial interests or personal relationships that could have appeared to influence the work reported in this paper.

Data availability

Data will be made available on request.

References

[1] Fellenius BH. Negative skin friction and settlement of piles. Singapore: Second International Seminar, Pile Foundations, Nanyang Technological Institute; 1984. p. 1–12. November.
[2] Sinha SK, Ziotopoulou K, Kutter BL. Centrifuge model tests of liquefaction-induced downdrag on piles in Uniform liquefiable deposits. J Geotech Geoenviron Eng 2022;139(9):04022048. https://doi.org/10.1061/(ASCE)GT.1943-5606.0002817.
[3] Sinha SK, Ziotopoulou K, Kutter BL. Displacement-based design of axially loaded piles for seismic loading and liquefaction-induced downdrag. J Geotech Geoenviron Eng 2023;149(9):1–15. https://doi.org/10.1061/JGGEFK.GTENG-11178.
[4] Boulanger RW, Brandenberg SJ. Neutral plane solution for liquefaction-induced downdrag on vertical piles. GeoTrans 2004:470–8. https://doi.org/10.1061/40744(154)32.
[5] Strand S. Liquefaction mitigation using vertical composite drains and liquefaction-induced downdrag on Piles : Implication for deep foundation design. Provo: UT:

Department of Civil and Environmental Engineering, Brigham Young University; 2008. Ph.D. Dissertation.
[6] Fellenius BH, Siegel TC. Pile drag load and downdrag in a liquefaction event. J Geotech Geoenviron Eng 2008;134(9):1412–6. https://doi.org/10.1061/(ASCE)1090-0241(2008)134:9(1412.
[7] Stringer ME, Madabhushi SPG. Re-mobilization of pile shaft friction after an earthquake. Can Geotech J 2013;50(9):979–88. https://doi.org/10.1139/cgj-2012-0261.
[8] Stringer ME, Madabhushi SPG. Axial load transfer in liquefiable soils for free-standing piles. Geotechnique 2013;63(5):400–9. https://doi.org/10.1680/geot.11.P.078.
[9] Rollins KM, Hollenbaugh J. Liquefaction induced negative skin friction from blast-induced liquefaction tests with auger-cast piles. In: Proc., *6th int. Conf. Earthq. Geotech. Eng.* Christchurch, New Zealand: international society for soil mechanics and geotechnical engineering; 2015.
[10] Vijayaruban VN, Muhunthan B, Fellenius BH. Liquefaction-induced downdrag on piles and drilled shafts. In: Proc., *6th int. Conf. On earthq. Geotech. Eng.* Christchurch, New Zealand: International Society for Soil Mechanics and Geotechnical Engineering; 2015.
[11] Muhunthan B, Vijayathasan NV, Abbasi B. Liquefaction-induced downdrag on drilled shafts. WA-RD 865.1. Pullman, WA: Washington State Department of Transportation; 2017.
[12] Rollins K. Dragload and downdrag on piles from liquefaction induced ground settlement. In: Bray JD, Boulanger RW, Cubrinovski M, Tokimatsu K, Kramer SL, O'Rourke T, Green RA, Robertson PK, Beyzaei CZ, editors. U.S.–New Zealand–Japan international workshop on liquefaction-induced ground movement effects. Berkeley, CA: Pacific Earthquake Engineering Research Center, University of California Berkeley; 2017. 2017/02.
[13] Nicks J. Liquefaction-induced downdrag on Continuous Flight Auger (CFA) piles from full-scale tests using blast liquefaction. FHWA-HRT-17-060. McLean, VA: Federal Highway Administration; 2017.
[14] Elvis I. Liquefaction-induced dragload and/or downdrag on deep foundations within the New Madrid seismic zone. Fayetteville, AR: University of Arkansas; 2018. Ph.D. Dissertation.
[15] Rollins KM, Amoroso S, Franceschini M. Liquefaction induced downdrag on full-scale micropile foundation. In: *Proc., 2nd int. Conf. On natural Hazards and infrastructure*. Chaina, Greece: innovation center for natural hazards and infrastructure; 2019.
[16] Fellenius BH, Abbasi B, Muhunthan B. Liquefaction induced downdrag for the juan pablo II bridge at the 2010 maule earthquake in Chile. Geotechnical Engineering Journal of the SEAGS & AGSSEA 2020;51(2):1–8.
[17] Lusvardi CM. Blast-induced liquefaction and downdrag development on a micropile foundation. Fayetteville, AR: Brigham Young University; 2020. Masters Thesis.
[18] Sinha SK, Ziotopoulou K, Kutter BL. Parametric study of liquefaction induced downdrag on axially loaded piles. In: 7th lnternational conference on earthquake geotechnical engineering. Rome, Italy: International Society for Soil Mechanics and Geotechnical Engineering; 2019. https://www.issmge.org/uploads/publications/59/104/ch565.pdf.
[19] Sinha SK, Ziotopoulou K, Kutter BL. SKS02: centrifuge test of liquefaction-induced downdrag in uniform liquefiable deposit. In: Centrifuge testing of liquefaction-induced downdrag on axially loaded piles. DesignSafe; 2021. https://doi.org/10.17603/ds2-d25m-gg48.
[20] Sinha SK, Ziotopoulou K, Kutter BL. SKS03: centrifuge test of liquefaction-induced downdrag in interbedded soil deposits. In: Centrifuge testing of liquefaction-induced downdrag on axially loaded piles. DesignSafe; 2021. https://doi.org/10.17603/ds2-wjgx-tb78.
[21] Sinha SK, Ziotopoulou K, Kutter BL. Centrifuge study of downdrag on axially loaded piles in liquefiable soils. In: 20th international Conference on soil mechanics and geotechnical engineering. Sydney, Australia: International Society for Soil Mechanics and Geotechnical Engineering; 2022. https://www.issmge.org/uploads/publications/1/120/ICSMGE_2022-595.pdf.
[22] Ziotopoulou K, Sinha SK, Kutter BL. Liquefaction-induced downdrag on piles: insights from a centrifuge and numerical modeling program. In: IVth international conference on performance based design in earthquake geotechnical engineering. Beijing, China: International Society of Soil Mechanics and Geotechnical Engineering; 2022.
[23] Sinha SK. Liquefaction-induced downdrag on piles: centrifuge and numerical modeling, and design procedures. Davis, CA: Department of Civil and Environmental Engineering, University of California Davis; 2022. Ph.D. Dissertation, https://escholarship.org/uc/item/7c0205nw.
[24] AASHTO (American Association of State Highway and Transportation Officials). AASHTO LRFD bridge design specifications. Washington, DC: AASHTO; 2020. LRFDUS-9.
[25] Knappett JA, Madabhushi SPG. Seismic bearing capacity of piles in liquefiable soils. Soils Found 2009;49(4):525–35. https://doi.org/10.3208/sandf.49.525.
[26] Sinha SK, Ziotopoulou K, Kutter BL. Numerical modeling of liquefaction-induced downdrag: validation against centrifuge model tests. J Geotech Geoenviron Eng 2022;148(12):04022111. https://doi.org/10.1061/(asce)gt.1943-5606.0002930.
[27] Winkler E. In: Domenicus H, editor. *Die Lehre von der Elastizität und Festigkeit* [*The systematic teaching of elasticity and strength*]; 1867. p. 182–4. Prague, Czechoslovakia.
[28] McKenna F, Scott MH, Fenves GL. Nonlinear finite-element analysis software architecture using object composition. J Comput Civ Eng 2010;24(1):95–107. https://doi.org/10.1061/(ASCE)CP.1943-5487.0000002.
[29] Garnier J, Gaudin C, Springman SM, Culligan PJ, Goodings D, Konig D, Kutter B, Phillips R, Randolph MF, Thorel L. Catalogue of scaling laws and similitude questions in geotechnical centrifuge modelling. Int J Phys Model Geotech 2007;7(3):1–23. https://doi.org/10.1680/ijpmg.2007.070301.
[30] Malvick EJ, Kulasingam R, Boulanger RW, Kutter BL. Effects of void redistribution on liquefaction flow of layered soil – centrifuge data report for EJM01. Davis, CA: Center for Geotechnical Modeling, University of California Davis; 2002. UCD/CGMDR-02/02, https://ucdavis.app.box.com/s/evhvz5tzz77bj9teutbr.
[31] Sinha SK, Kutter BL, Wilson DW, Carey T, Ziotopoulou K. Use of Photron cameras and TEMA software to measure 3D displacements in centrifuge tests. UCD/CGM-21/01, Center for Geotechnical Modeling. University of California Davis; 2021. https://escholarship.org/uc/item/830502mm.
[32] Sinha SK, Kutter BL, Ziotopoulou K. Measuring vertical displacement using laser lines and cameras. Int J Phys Model Geotech 2021:1–13. https://doi.org/10.1680/jphmg.21.00038.
[33] Sinha SK, Kutter BL, Ziotopoulou K. Using cameras for measuring displacements in model tests. In: Proc 10th international conference on physical modeling in geotechnics (ICPMG); 2022. Daejon, Korea, https://escholarship.org/uc/item/1fd8r504.
[34] Boulanger RW, Curras CJ, Kutter BL, Wilson DW, Abghari A. Seismic soil-pile-structure interaction experiments and analyses. J Geotech Geoenviron Eng 1999;125(9):750–9. https://doi.org/10.1061/(ASCE)1090-0241(1999)125:9(750.
[35] Sinha SK, Ziotopoulou K, Kutter BL. Effects of excess pore pressure redistribution on liquefiable layers. J Geotech Geoenviron Eng 2024;149(9):1–15. https://doi.org/10.1061/JGGEFK.GTENG-11178.